

Published in final edited form as:

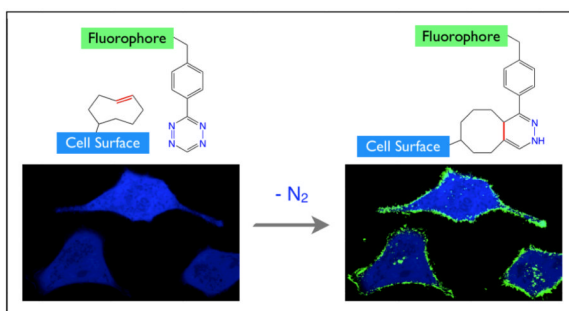
*Acc Chem Res.* 2011 September 20; 44(9): 816–827. doi:10.1021/ar200037t.

## Biomedical Applications of Tetrazine Cycloadditions

 Neal K. Devaraj<sup>1,\*</sup> and Ralph Weissleder<sup>1,2,\*</sup>
<sup>1</sup>Center for Systems Biology, Massachusetts General Hospital, 185 Cambridge St, CPZN 5206, Boston, Massachusetts 02114, USA

<sup>2</sup>Department of Systems Biology, Harvard Medical School, 200 Longwood Avenue, Boston, Massachusetts 02115, USA

### Conspectus



Disease mechanisms are increasingly being resolved at the molecular level. Biomedical success at this scale creates synthetic opportunities for combining specifically designed orthogonal reactions in applications such as imaging, diagnostics, and therapy. For practical reasons, it would be helpful if bioorthogonal coupling reactions proceeded with extremely rapid kinetics ( $k > 10^3 \text{ M}^{-1} \text{ sec}^{-1}$ ) and high specificity. Improving kinetics would minimize both the time and amount of labeling agent required to maintain high coupling yields. In this Account, we discuss our recent efforts to design extremely rapid bioorthogonal coupling reactions between tetrazines and strained alkenes.

These selective reactions were first used to covalently couple conjugated tetrazine near-infrared-emitting fluorophores to dienophile-modified extracellular proteins on living cancer cells. Confocal fluorescence microscopy demonstrated efficient and selective labeling, and control experiments showed minimal background fluorescence. Multistep techniques were optimized to work with nanomolar concentrations of labeling agent over a timescale of minutes: the result was successful real-time imaging of covalent modification. We subsequently discovered fluorogenic probes that increase in fluorescence intensity after the chemical reaction, leading to an improved signal-to-background ratio. Fluorogenic probes were used for intracellular imaging of dienophiles. We further developed strategies to react and image chemotherapeutics, such as *trans*-cyclooctene taxol analogs, inside living cells. Because the coupling partners are small molecules (<300 daltons), they offer unique steric advantages in multistep amplification.

We also describe recent success in using tetrazine reactions to label biomarkers on cells with magneto-fluorescent nanoparticles. Two-step protocols that use bioorthogonal chemistry can significantly amplify signals over both one-step labeling procedures as well as two-step procedures that use more sterically hindered biotin–avidin interactions. Nanoparticles can be detected with fluorescence or magnetic resonance techniques. These strategies are now being

\*ndevaraj@mgh.harvard.edu, rweissleder@mgh.harvard.edu .

routinely used on clinical samples for biomarker profiling to predict malignancy and patient outcome.

Finally, we discuss recent results with tetrazine reactions used for in vivo molecular imaging applications. Rapid tetrazine cycloadditions allow modular labeling of small molecules with the most commonly used positron emission tomography isotope,  $^{18}\text{F}$ . Additionally, in recent work we have begun to apply this reaction directly in vivo for the pre-targeted imaging of solid tumors. Future work with tetrazine cycloadditions will undoubtedly lead to optimized protocols, improved probes, and additional biomedical applications.

## Introduction

Bioorthogonal covalent reactions have found widespread use in chemical biology.<sup>1</sup> Applications include the tracking of metabolite analogs, activity-based protein profiling, target guided synthesis of enzyme inhibitors, and imaging small molecules in live cells and animals.<sup>2-5</sup> A variety of covalent reactions have been used as irreversible chemoselective coupling tools. Notable examples include the Staudinger ligation and the copper catalyzed or strain-promoted azide-alkyne cycloadditions (often referred to as “click” chemistry).<sup>6-9</sup> We became interested in utilizing such orthogonal reactions to assemble imaging agents, nanomaterials, and therapeutics in the presence of live cells both in vitro for microscopy and diagnostic application, as well as in vivo.

Unfortunately many conventional bioorthogonal coupling reactions suffer from slow kinetics ( $k < 1 \text{ M}^{-1}\text{sec}^{-1}$ ) compared to non-covalent affinity ligands ( $k_{\text{on}} \sim 10^5\text{-}10^6 \text{ M}^{-1}\text{sec}^{-1}$ ).<sup>2,9,10</sup> Such sluggish kinetics are likely to be problematic when using micro-nanomolar concentrations of labeling agent, which is often the case in vivo. One way to illustrate this point is to consider a reaction between 1 micromolar of labeling agent in solution and a surface bound coupling partner. Assuming the reaction follows pseudo-first order kinetics (due to the large excess of solution species compared to the surface restricted species) and the second order rate constant for reaction was  $1 \text{ M}^{-1}\text{sec}^{-1}$ , the surface coupling would take approximately eight days for fifty-percent completion. Of course, increasing the concentration of labeling agent would speed this reaction up proportionally. However oftentimes it is neither practical nor possible to achieve very high concentrations of coupling agents, for instance when using nanomaterials, performing reactions in vivo, or when using radionuclide imaging agents.

With this kinetic limitation in mind, we and others have explored alternative cycloadditions that react with rapid kinetics and can be performed under biologically relevant conditions and in the presence of biological functional groups. Among the many reactions reported, the inverse electron demand cycloaddition between 1,2,4,5 tetrazines and strained dienophiles such as norbornene, cyclooctyne, and *trans*-cyclooctene has emerged as a valuable bioorthogonal coupling tool.<sup>11-14</sup> These reactions can be extremely fast, do not require a catalyst, and work well in aqueous solutions and serum. Furthermore, the coupling partners do not require tedious multistep synthesis. In this account we describe recent work by our group and others to explore rapid tetrazine cycloadditions for applications in cellular microscopy, clinical point-of-care diagnostics, and in vivo imaging.

## Tetrazine Inverse Electron Demand Diels-Alder Cycloadditions

Tetrazine syntheses have been reported in the literature since the late 19th century. Pinner reported the first synthesis after he reacted equimolar quantities of hydrazine and benzonitrile and, after mild oxidation, isolated a red compound to which he properly assigned the formula for 3,6-diphenyl-*s*-tetrazine.<sup>15,16</sup> Though he reported several variants,

he did not investigate their properties in great detail. While studying the synthesis of tetrazines from fluoroolefins and hydrazine, Carboni and Lindsey discovered that tetrazines reacted readily with a variety of unsaturated compounds releasing one mole of nitrogen and yielding either dihydropyridazines or pyridazines depending on the dienophile reactant.<sup>17</sup> It has since been determined that tetrazines react through a formal [4+2] Diels-Alder cycloaddition with numerous dienophiles (Figure 1). The adduct (which has not been observed) immediately undergoes an irreversible retro Diels-Alder step, which is responsible for the release of nitrogen.<sup>16</sup> Reaction with alkynes leads to pyridazines while reaction with olefins typically leads to rearrangement and the formation of dihydropyridazines.

Tetrazine reaction with dienophiles can be followed spectroscopically by observing the disappearance of the visible absorption band usually found between 510-550 nm. Using this technique, Sauer performed extensive kinetic studies of the cycloaddition of various 1,2,4,5 substituted tetrazines with numerous dienophiles.<sup>18-20</sup> These reactions were typically performed in dioxane at room temperature. From this valuable data several trends emerged. There is great variance in the reaction rate constant which can vary over 9 orders of magnitude depending on the dienophile. Internal olefins react extremely sluggishly (an important requirement for a bioorthogonal reaction as internal *cis*-alkenes are prevalent in cellular membranes). Strain has a tremendous effect on reaction rate constant. For instance, Sauer reported a rate constant of  $12700 \text{ M}^{-1}\text{sec}^{-1}$  for the highly strained olefin *trans*-cyclooctene at 20°C in dioxane.<sup>19</sup> In contrast, *cis*-cyclooctene was reported to react with a rate constant of  $0.03 \text{ M}^{-1}\text{sec}^{-1}$  under the same conditions. Although Sauer's results were in dioxane, more recent work had established that the reaction can be performed in aqueous solution.<sup>21</sup> In fact, the addition of water increases the rate constant for the reaction.

The reported rapid kinetics and ability to perform the reaction in water attracted our group, and others, to the promise of this type of reaction for bioorthogonal couplings<sup>11,12</sup>. We therefore decided to start a program exploring the applicability of this reaction to live cell labeling.

## Multistep Labeling of Live Cell Surface Antigens

In order to test the applicability of tetrazine dienophile cycloadditions for bioorthogonal couplings, we first synthesized a benzylamino-tetrazine. This tetrazine showed excellent stability in aqueous buffer with negligible degradation after prolonged standing at room temperature. In serum, the tetrazine showed good stability, retaining approximately 85% activity after 15 hours at 20°C.<sup>11</sup> Cycloaddition between the tetrazine and the commercially available dienophile norbornene carboxylic acid proceeded in greater than 93% yield and with a rate constant of approximately  $1.9 \text{ M}^{-1}\text{sec}^{-1}$  in aqueous buffer. Additionally, a reaction rate constant of  $1.6 \text{ M}^{-1}\text{sec}^{-1}$  was measured in serum.

Labeling of specific functional groups on live cells has emerged as a powerful application of bioorthogonal couplings. We were therefore interested in demonstrating tetrazine live cell labeling by performing multistep modification of antibodies pre-bound to surface antigens. Such multistep techniques could provide novel methods to increase signal-to-background both for in vivo and in vitro diagnostics. To demonstrate the utility of the tetrazine–norbornene reaction for antibody targeted live cell labeling, we used the monoclonal antibody trastuzumab (Herceptin) which binds to Her2/neu growth factor receptors. Trastuzumab lysine residues were simultaneously labeled with norbornene and tetramethyl rhodamine using standard amine coupling reactions. Human breast cancer SKBR3 cells, which overexpress Her2/neu, were incubated with 200 nM norbornene-antibody, and then treated with 50  $\mu\text{M}$  of a tetrazine conjugated to a near-infrared emitting fluorescent probe for 30 min at 37 °C. After washing, the cells were imaged using both rhodamine and near-

infrared fluorescence channels. Significant labeling, which colocalizes, was observed in both channels. Cells incubated with a control antibody, which contained rhodamine but not norbornene, showed insignificant infrared signal after exposure to the tetrazine probe. These experiments demonstrated the specificity of the tetrazine imaging agent for norbornene-modified antibody in the presence of live cells and serum.

Simultaneous to our work, the Fox group, following the work of Sauer, demonstrated that dipyrrolic tetrazines could react with highly strained *trans*-cyclooctenes in water or standard cell nutrient media.<sup>12</sup> The bimolecular rate constants reported were approximately  $2,000 \text{ M}^{-1}\text{sec}^{-1}$  at room temperature. The reaction was performed between a tetrazine and thioredoxin *trans*-cyclooctene conjugate to demonstrate bioconjugation and the feasibility of using the reaction to modify proteins with useful functional groups. Unfortunately, the tetrazine employed was highly reactive, degrading by 20% in water after 2 hours and 50% after exposure to 20 mM of thiols for 10 minutes.

Although dipyrrolic tetrazines appeared unsuitable for prolonged live cell or in vivo imaging applications, we were impressed with the reported rapid cycloaddition kinetics of *trans*-cyclooctene. We therefore decided to determine how fast *trans*-cyclooctenes reacted with the more stable benzylamino-tetrazine we had synthesized (Figure 2A).<sup>14</sup> Studying surface reactions, we determined a rate constant of approximately  $6000 \text{ M}^{-1}\text{sec}^{-1}$  at  $37^\circ\text{C}$  between fluorophore conjugated tetrazine and *trans*-cyclooctene conjugated to a monoclonal antibody. Similar to our previous work with tetrazine norbornene cycloadditions, we decided to apply the tetrazine *trans*-cyclooctene reaction to multistep assembly of imaging agents on live cells (Figure 2B). For cell labeling studies, we chose to target epidermal growth factor receptor (EGFR) given its central importance in cancer, cell signaling, and as a key target for therapeutic inhibition.<sup>22,23</sup> Commercially available anti-EGFR (Cetuximab) monoclonal antibodies were modified using amine reactive *trans*-cyclooctenes and used for imaging experiments.<sup>24</sup> As a cancer model, we worked with a green fluorescent protein (GFP) expressing A549 lung cancer cell line which was shown to have upregulated levels of EGFR.<sup>25</sup> To label cells displaying *trans*-cyclooctene bearing antibodies, benzylamino-tetrazine was once again conjugated to a near-infrared emitting fluorophore.

Initial labeling experiments used Cetuximab modified by *trans*-cyclooctene and a single Alexafluor 555 dye in order to determine if sequential tetrazine-near infrared labeling colocalized with antibody. A549 cancer cells were first incubated with 100 nM Cetuximab *trans*-cyclooctene/AF555. In contrast to our work with norbornene antibodies, where cells were incubated for 30 minutes with 50  $\mu\text{M}$  tetrazine probe, cells were instead incubated at  $37^\circ\text{C}$  with 500 nM tetrazine probe for 10 minutes in 100% serum. After washing, the cells were immediately imaged using confocal microscopy (Figure 3). Antibodies were imaged in the red channel and localized both on the surfaces of the cells and inside due to EGFR internalization. Covalently bound tetrazine dyes were readily visualized in the near-infrared channel. Merging the red and near-infrared channels revealed excellent colocalization of the antibody and tetrazine related signals with little background indicating that the tetrazine *trans*-cyclooctene reaction was extremely selective. As expected, reaction occurred primarily on the surface of the cells. Control experiments using either antibody lacking *trans*-cyclooctene or near-infrared dyes lacking tetrazine resulted in very little observable fluorescent signals.

We also tested if labeling could be observed without a washing step. This may be relevant to applications where one is unable to perform stringent and multiple washing steps, such as experiments in which cell handling has to be minimized due to cell rarity or sensitivity. The concentration of the tetrazine near-infrared probe was lowered to just 50 nM in order to observe the covalent modification in real time. Figure 4 depicts several panels taken from

continuous imaging of the tetrazine cycloaddition to *trans*-cyclooctene localized on the surface of live cancer cells in serum containing 50 nM tetrazine probe. The near-infrared probe became visible as it reacted on the surface of cells, and at later times, punctate spots within the cell were visible as tetrazine labeled proteins were internalized.

## Imaging Small Molecules Inside of Living Cells with Fluorogenic Tetrazines

Although there have been several examples of using bioorthogonal reactions to image molecules on the surfaces of living cells, the use of bioorthogonal reactions to image small molecules inside of living cells has been extremely limited.<sup>26</sup> The reasons for this are likely several. In addition to fulfilling stability, toxicity, and chemoselectivity requirements, intracellular live cell labeling requires reagents that can easily diffuse through biological membranes and kinetics that enable rapid labeling even with the low concentrations of agent that do make it across the membrane. Impressed with the rapid kinetics of the tetrazine *trans*-cyclooctene reaction, we were interested in examining its utility for labeling and imaging molecules inside of live cells.

To explore intracellular tetrazine labeling, we conjugated 3-(4-benzylamino)-1,2,4,5-tetrazine to commercially available succinimidyl esters of visible light emitting boron-dipyrromethene (BODIPY) dyes.<sup>13</sup> BODIPY dyes are uncharged and lipophilic and, for these reasons, have seen use in numerous intracellular applications.<sup>27-29</sup> We also wondered whether or not these visible fluorophores would show electronic interactions with the tetrazine chromophores, which have absorption maxima at 510-530 nm. In fact, the tetrazine BODIPY conjugates exhibited strongly reduced fluorescence compared to the parent succinimidyl esters of the fluorophores. Upon reaction with a strained dienophile, such as *trans*-cyclooctenol, the fluorescence was “switched” back on (Figure 5). The fluorogenic nature of these probes had important implications for the feasibility of intracellular imaging. A practical intracellular bioorthogonal coupling scheme would likely need to incorporate a fluorogenic mechanism to avoid visualizing accumulated but unreacted imaging agent (i.e. “background”). Such activatable “turn-on” probes would significantly increase the signal-to-background ratio, which is particularly relevant to imaging targets inside living cells since a stringent washout of unreacted probe is extremely difficult.

Tetrazine quenching was efficient for probes emitting between 510 and 570 nanometers. Tetrazine conjugates of commercially available succinimidyl esters of BODIPY FL, BODIPY TMR-X, and Oregon Green 488 all showed excellent quenching and between 15-20 fold increase in fluorescence after reaction with *trans*-cyclooctene. However, conjugates of lower or higher wavelength dyes showed much lower quenching. Our previously used tetrazine near-infrared dye had no observable fluorogenic property, explaining why we had not noticed the phenomenon earlier. The quenching was pH independent and was observed in buffer or pure serum. The strong wavelength dependence of quenching had led us to hypothesize that the mechanism involved resonance energy transfer between fluorophore and the tetrazine chromophore which absorbs between 510-530 nm. Recently, Miomandre and coworkers have performed extensive analysis of quenched BODIPY tetrazines and came to the conclusion that quenching is in fact mainly due to energy transfer.<sup>30</sup>

To test the applicability of these fluorogenic probes for intracellular imaging, we initially imaged extracellular and intracellular distributions of *trans*-cyclooctene tagged monoclonal antibodies (Figure 6). A431 human epithelial carcinoma cells were exposed to 100 nM of *trans*-cyclooctene tagged Cetuximab. One population of cells was incubated for 1 hour at 4°C to minimize internalization of antibody. A second group of cells was incubated for 1 hour at 37°C to promote internalization. After incubation, the cells were first exposed to 1



$\mu\text{M}$  of a highly charged tetrazine near-infrared conjugate that we knew, from prior experience, had difficulty diffusing through cell membranes. After washing, in a second step the cells were exposed to  $1 \mu\text{M}$  of tetrazine BODIPY-FL, the cell permeable lipophilic turn-on probe. Multicolor imaging in the near-infrared (green) and BODIPY (red) channels revealed very little internalized antibody in the cells incubated at  $4^\circ\text{C}$ . However, imaging the cells incubated at  $37^\circ\text{C}$  revealed numerous populations of internalized antibodies, presumably located in endosomes.

Encouraged by our ability to image intracellular *trans*-cyclooctene antibody conjugates, we wondered whether or not a similar technique could be used to track *trans*-cyclooctene tagged small molecules inside of cells. Such a technique could find application in determining in vitro or in vivo subcellular distributions of pharmaceutical analogs containing a dienophile tag. It might also provide an alternative to radiolabeling for tracking small molecule distributions. Radionuclide based techniques suffer from cost, radiation hazard, and poor spatial resolution of the resulting images. As an initial molecular target, we synthesized a *trans*-cyclooctene modified paclitaxel (Taxol®).<sup>13</sup> Taxol was selected because of its tremendous clinical use and the large body of prior work that serves as reference.<sup>31</sup> The dienophile was introduced in the C7 position since prior structure activity relationship studies have established that modifications at the C7 position do not significantly affect the biological activity of taxol<sup>32,33</sup>. Indeed, *trans*-cyclooctene taxol was capable of polymerizing tubulin in a manner similar to that of native taxol.

For live cell studies, kangaroo rat kidney cells were incubated in cell media containing  $1 \mu\text{M}$  *trans*-cyclooctene taxol for 1 hour at  $37^\circ\text{C}$ . After washing, cells were exposed to media containing  $1 \mu\text{M}$  tetrazine-BODIPY FL for 20 minutes at room temperature. The cells were then washed and imaged using confocal microscopy (Figure 7). Structures reflecting intracellular *trans*-cyclooctene/tetrazine conjugate distributions become readily apparent. Control experiments employing tetrazine-BODIPY FL alone or with unmodified taxol yielded minimal fluorescence background signal and demonstrate that there is little non-specific or background turn-on and that the images result from the specific tetrazine *trans*-cyclooctene cycloaddition reaction. Furthermore, cells treated with *trans*-cyclooctene modified taxol followed by a highly charged non-membrane permeable tetrazine near-infrared probe showed insignificant staining, giving further evidence that tetrazine-BODIPY FL is able to penetrate the cell membrane and label *trans*-cyclooctene located within the cell.

## Modifying Cells with Nanomaterials for Clinical Diagnostics

Our initial work exploring tetrazine cycloadditions focused on labeling cells using fluorescent small molecule probes. However, we realized that this technique, in principal, could be applied to other diagnostic probes. We have had long standing interest in using magnetic nanoparticles to separate and profile biomarkers in diseased tissue.<sup>34-36</sup> Magnetic based sensing schemes benefit from high sensitivity, low cost, and the ability to perform measurements in samples that are not optically transparent. In order to bring biomarker selectivity, nanoparticles are often conjugated to monoclonal antibody affinity agents. The synthesis and purification of such conjugates is not trivial. Typical coupling schemes use multivalent reactive groups on both nanoparticles and antibodies, and this can often lead to cross-linking and aggregation. Nanoparticles and antibodies are both very large macromolecular entities. Purification typically requires gel filtration chromatography and even then it is difficult to achieve efficient separation. Additionally, we were interested in maximizing the signal per antigen by increasing the number of nanoparticles per antibody. Unfortunately, antibodies decorated with multiple nanoparticles oftentimes have poor stability, crashing out of solution.<sup>35,37</sup> Furthermore, multiple nanoparticles on a single

antibody can lead to blocking of the site of antigen binding lowering the affinity of the conjugate.

We initially tested whether or not *trans*-cyclooctene modified antibodies could be modified by tetrazine modified magneto-fluorescent nanomaterials (Figure 8A).<sup>38,39</sup> As expected, conjugation took place rapidly when the reactive precursors were exposed to one another. These constructs could then be used to directly label cell surfaces for biomarker profiling. However, in this direct labeling scheme, the bioorthogonal reaction between tetrazines and dienophiles was simply used as any other conjugation chemistry. As opposed to the one step scheme, we also envisioned a two step protocol where cells were first exposed to dienophile laden antibody, with the choice of antibody dependent on the biomarker of interest (Figure 8B). In a second step, the cells would be exposed to a universal tetrazine magneto-fluorescent nanoparticle. This two step protocol had several envisioned advantages. Synthetically, it is straightforward to conjugate small molecules to macromolecules and separate via low molecular weight cutoff centrifugation filtration. Additionally, we imagined there might be amplification of signal through maximizing the loading of nanomaterials per antibody. There would be no fear of stability as the antibodies would already effectively be “crashed” out of solution and bound to cell surfaces. Additionally, since the antibodies would be reacted after being bound to antigen, it would be unlikely that a nanomaterial would be able to sterically block the site of binding.

Using the two step format, we determined how *trans*-cyclooctene modification of antibodies promotes nanoparticle binding. We initially targeted three biomarkers, EGFR, EPCAM, and HER2 that were chosen based on their relevance to cancer. By exposing antibodies to varying concentrations of an amine-reactive *trans*-cyclooctene the antibody *trans*-cyclooctene valencies could be varied between approximately one and 30 per antibody. Following sequential incubations with *trans*-cyclooctene-antibody and tetrazine-magnetofluorescent nanoparticle, we found that nanoparticle binding increased with successive *trans*-cyclooctene loading until saturating.<sup>38</sup> Dienophile modifications had little effect on anti-HER2 affinity until loading levels reached 30 *trans*-cyclooctene per antibody. This likely reflects an advantage of using a small molecule coupling partner with a minimum steric footprint. Live cells modified with magnetofluorescent nanoparticles using this two step protocol could also be imaged using confocal fluorescence microscopy.

Compared to the one-step method, we found that the two step method consistently led to much higher nanoparticle loadings on cells. In most cases, the signals were amplified by a factor of 10 when using 100 nM of nanoparticle. We believe this result was due to several factors. Part of the amplification was no doubt due to the high valencies and small sizes of the reactants which promoted attachment of multiple nanoparticles to each antibody scaffold. This amplified the signal per biomarker. An additional hypothesis is that direct antibody nanoparticle conjugates had the potential to cross-link multiple markers, which could lead to a less than a 1:1 ratio of nanoparticle per marker. Because the *trans*-cyclooctene antibody was applied in excess before nanoparticle exposure and contained numerous dienophile moieties, most marker sites should be occupied by separate antibody scaffolds, and cross-linking of neighboring antibodies by a nanoparticle would consume an additional dienophile rather than an entire marker.

To determine whether the amplification was unique to the small molecule chemistry applied or simply a consequence of using a two-step labeling strategy, we also tested a multistep strategy that used avidin/biotin interactions for coupling.<sup>38</sup> Although multistep nanoparticle binding using avidin/biotin exceeded the single step use of direct antibody-nanoparticle conjugates, the overall signal remained considerably lower compared to tetrazine *trans*-cyclooctene multistep labeling (Figure 9). We speculate that this finding can be attributed to

the large size of avidin, which could potentially mask adjacent biotin sites.<sup>40</sup> Additionally, biotin must associate within a deep cleft inside the avidin protein, which could physically or spatially constrain certain binding configurations. These results highlighted specific advantages that can be obtained when using rapid small molecule bioorthogonal chemistry that cannot be reproduced using biological conjugation strategies.

Currently the tetrazine-magnetic nanoparticle multistep technique is being used in our center to profile dozens of different biomarkers using portable diagnostic magnetic resonance sensors. We have also adapted the technique for the detection of intracellular biomarkers. Recently we implemented the technology in a clinical setting to analyze harvested cells from 70 patients.<sup>41</sup> Single fine needle aspirates yielded sufficient numbers of cells to quantitate nine cancer related protein markers in all patients. Accuracies reached 96% for establishing cancer diagnoses, surpassing those of conventional analyses and demonstrating the power of quantitative profiling. This point-of-care technique may enhance our current molecular diagnostic capabilities.

In addition to utility with magnetic nanomaterials, in collaboration with the Bawendi group, we have also demonstrated that tetrazine chemistry is very suitable for bioorthogonal modification of fluorescent cadmium based nanocrystals or “quantum dots.”<sup>42</sup> Copper catalyzed azide-alkyne cycloadditions are incompatible with quantum dots since trace quantities of copper ions irreversibly quench nanoparticle fluorescence.<sup>42</sup> Tetrazine/dienophile cycloadditions do not require metal ion catalysts, and quantum dots coated with a norbornene polymer could be readily modified with tetrazine containing dyes and proteins with negligible change in fluorescence.

## In Vivo Imaging Applications

Although our initial work focused on proof of concept in vitro demonstrations, we have begun to explore in vivo imaging applications. An initial application was the use of tetrazine reactions to rapidly and irreversibly tag small molecules with radionuclides such as <sup>18</sup>F. The <sup>18</sup>F radionuclide is a widely available positron emission tomography (PET) isotope that is produced daily in cyclotrons at most major hospitals and distributions centers. The addition of <sup>18</sup>F to functionally complex materials is chemically challenging and this challenge is exacerbated by its short radioactive half-life of approximately 110 minutes. For these reasons, facile <sup>18</sup>F platform type labeling strategies are very attractive.

We and others have explored the use of <sup>18</sup>F *trans*-cyclooctene as a reactive platform that can rapidly introduce a PET radionuclide to a given tetrazine small molecule.<sup>43,44</sup> We synthesized an <sup>18</sup>F modified *trans*-cyclooctene from a readily prepared tosylate precursor in 44% decay corrected radiochemical yield and in greater than 93% radiochemical purity. Following earlier work with PARP1 inhibitors, we designed a tetrazine analog of the PARP1 inhibitor AZD2281.<sup>45</sup> The tetrazine-AZD2281 reacted with <sup>18</sup>F *trans*-cyclooctene over three minutes and, after high performance liquid chromatography purification, yielded <sup>18</sup>F tagged AZD2281 adducts in 59.6% isolated decay corrected radiochemical yield and in greater than 96% radiochemical purity (Figure 10A). Attempts to directly fluorinate an AZD2281 analog led to decomposition or much lower radiochemical yields, demonstrating the power of the bioorthogonal platform approach.

The use of highly reactive tetrazine/*trans*-cyclooctene chemistry has the additional advantage that excess cold AZD2281 tetrazine can be removed within minutes using a *trans*-cyclooctene scavenger resin.<sup>46</sup> This serves as a faster alternative to chromatographic purification and could prove useful for molecules where the cold electrophilic precursor and <sup>18</sup>F product are difficult to separate. Our novel <sup>18</sup>F AZD2281 probe was successfully



tested in biological assays and its potency and targeted accumulation was confirmed in vivo with mice bearing breast cancer tumor xenografts (Figure 10B).

There has also been progress both in our lab and others in using the reaction directly in vivo. In vivo multistep reaction of tetrazine small molecule imaging agents to *trans*-cyclooctene pretargeted antibodies could provide better signal-to-background compared to directly labeled antibodies, which clear too slowly due to their high molecular weight.<sup>47</sup> Following our work with multistep labeling of antibody targeted cancer cells in vitro, Phillips research reported successful in vivo labeling of antibody modified xenografts using a multistep approach.<sup>48</sup> The group injected a *trans*-cyclooctene anti-TAG72 antibody into mice bearing a colon cancer tumor xenograft. After waiting 24 hours to allow for clearance, they injected an indium-111 labeled tetrazine small molecule. Due to its low molecular weight, this tetrazine chaser showed rapid renal clearance. The chaser was allowed to react in vivo for three hours prior to imaging and analysis. Tumor to muscle ratios of approximately 13 were reported as were single photon emission computed tomography (SPECT) images. However, the half-life of indium-111 is 2.8 days, so one could have alternatively injected antibodies directly modified with indium-111 and simply waited for antibody clearance. Furthermore, the amount of tetrazine injected in the second step was high (>20  $\mu\text{g}$  of small molecule). Although tetrazine cycloadditions are well established for in vitro labeling, further work will be needed before routine in vivo application.

## Conclusions/Outlook

Tetrazine cycloadditions have proven to be a new bioorthogonal covalent coupling tool. The main advantages of this reaction compared to conventional bioorthogonal reactions are the following: there is no requirement of a catalyst; the bimolecular rate constants for reaction can be very high ( $>10^3 \text{ M}^{-1}\text{sec}^{-1}$ ) with appropriate choice of tetrazine and strained dienophile; certain tetrazine fluorophores are fluorogenic upon cycloaddition thus improving signal-to-background for fluorescence microscopy; the reactants are straightforward to synthesize from commercial sources. There are still some disadvantages to the reaction compared to conventional azide/alkyne or Staudinger ligations. Perhaps most notably, the reactants, though small molecules, are still larger than an azide or terminal acetylene (3 atoms). This will likely prevent the introduction tetrazines or strained dienophiles such as *trans*-cyclooctene onto metabolite scaffolds while still allowing them to be utilized by the biosynthetic machinery of living cells. Additionally the reaction is not regioselective or stereoselective. However, for labeling applications, this is not problematic as all isomers couple the tetrazine to the dienophile.

The rapid kinetics of tetrazine cycloadditions have proven quite advantageous. The labeling of live cells with tetrazine fluorophores proceeded in minutes with nanomolar concentration of probe. Intracellular imaging was also feasible and was aided by the discovery of fluorogenic tetrazine probes. The rapid reaction between small molecules with favorable steric footprints allowed large amplification in multistep assembly of nanomaterials for diagnostic applications. Finally, we and others have begun probing the application of the reaction for in vivo imaging particular with respect to the assembly of radionuclide probes. Our early work has demonstrated that the rapid kinetics of tetrazine cycloadditions allows utility for a variety of bioimaging and nanoparticle applications. We are extremely confident that future work with tetrazine cycloadditions will refine current approaches and uncover additional biomedical applications.

## Acknowledgments

The authors gratefully acknowledge S. A. Hilderbrand, J. B. Haun, G. M. Thurber, C. Castro, T. Reiner, N. Keliher, R. Mazitschek for their contributions to the above discussed research as well as for their many helpful discussions and suggestions. This work was funded in part by NIH grants P50CA86355, R01EB010011, K01EB010078 and T32CA079443.

## Biography

Neal K. Devaraj: Dr. Devaraj performed his undergraduate studies at MIT and obtained a PhD in Chemistry from Stanford University under the mentorship of James Collman and Christopher Chidsey. At Stanford he developed techniques to covalently modify electrode surfaces with redox probes and multielectron redox catalysts. Since 2007 he has been at the Harvard Medical School (HMS), first as a postdoctoral fellow with Ralph Weissleder, and currently as an Instructor of Medicine. During his time at HMS he has explored the use of cycloadditions for in-situ assembly of imaging and diagnostic agents in the presence of live cells and in vivo. His work has been recognized with several awards including an American Chemical Society Young Investigator Award and a National Institutes of Health Career Development Award.

Ralph Weissleder: Dr. Weissleder is a Professor at Harvard Medical School, Director of the Center for Systems Biology at Massachusetts General Hospital (MGH), and Attending Clinician (Interventional Radiology) at MGH. He graduated from the University of Heidelberg, and has been faculty at HMS since 1991. He has published over 600 publications in peer reviewed journals and has authored several textbooks. His work has been honored with numerous awards including the J. Taylor International Prize in Medicine, the Millenium Pharmaceuticals Innovator Award, the AUR Memorial Award, the ARRS President's Award, The Society for Molecular Imaging Lifetime Achievement Award, and the Academy of Molecular Imaging 2006 Distinguished Basic Scientist Award. In 2009 he was elected member of the US National Academies Institute of Medicine. His lab has developed systematic ways to explore disease biology using in vivo imaging and has been instrumental in translating several discoveries into new drugs.

## References:

1. Prescher JA, Bertozzi CR. Chemistry in living systems. *Nat Chem Biol.* 2005; 1:13–21. [PubMed: 16407987]
2. Baskin JM, et al. Copper-free click chemistry for dynamic in vivo imaging. *Proc Natl Acad Sci U S A.* 2007; 104:16793–16797. [PubMed: 17942682]
3. Speers AE, Adam GC, Cravatt BF. Activity-based protein profiling in vivo using a copper(i)-catalyzed azide-alkyne [3 + 2] cycloaddition. *J Am Chem Soc.* 2003; 125:4686–4687. [PubMed: 12696868]
4. Lewis WG, et al. Click chemistry in situ: acetylcholinesterase as a reaction vessel for the selective assembly of a femtomolar inhibitor from an array of building blocks. *Angew. Chem. Int. Ed.* 2002; 41:1053–1057.
5. Laughlin ST, Baskin JM, Amacher SL, Bertozzi CR. In vivo imaging of membrane-associated glycans in developing zebrafish. *Science.* 2008; 320:664–667. [PubMed: 18451302]
6. Saxon E, Bertozzi CR. Cell surface engineering by a modified Staudinger reaction. *Science.* 2000; 287:2007–2010. [PubMed: 10720325]
7. Rostovtsev VV, Green LG, Fokin VV, B. SK. A stepwise Huisgen cycloaddition process: Copper (I)-catalyzed regioselective “ligation” of azides and terminal alkynes. *Angew. Chem. Int. Ed.* 2002; 41:2596–2599.
8. Kolb HC, Finn MG, Sharpless KB. Click Chemistry: Diverse Chemical Function from a Few Good Reactions. *Angew. Chem. Int. Ed.* 2001; 40:2004–2021.

9. Agard NJ, Prescher JA, Bertozzi CR. A strain-promoted [3 + 2] azide-alkyne cycloaddition for covalent modification of biomolecules in living systems. *J Am Chem Soc.* 2004; 126:15046–15047. [PubMed: 15547999]
10. Ning XH, Guo J, Wolfert MA, Boons GJ. Visualizing metabolically labeled glycoconjugates of living cells by copper-free and fast Huisgen cycloadditions. *Angew. Chem. Int. Ed.* 2008; 47:2253–2255.
11. Devaraj NK, Weissleder R, Hilderbrand SA. Tetrazine-Based Cycloadditions: Application to Pretargeted Live Cell Imaging. *Bioconjug Chem.* 2008; 19:2297–2299. [PubMed: 19053305]
12. Blackman ML, Royzen M, Fox JM. Tetrazine ligation: fast bioconjugation based on inverse-electron-demand Diels-Alder reactivity. *J Am Chem Soc.* 2008; 130:13518–13519. [PubMed: 18798613]
13. Devaraj NK, Hilderbrand S, Upadhyay R, Mazitschek R, Weissleder R. Bioorthogonal Turn-On Probes for Imaging Small Molecules inside Living Cells. *Angew. Chem. Int. Ed.* 2010; 49:2869–2872.
14. Devaraj NK, Upadhyay R, Haun JB, Hilderbrand SA, Weissleder R. Fast and sensitive pretargeted labeling of cancer cells through a tetrazine/trans-cyclooctene cycloaddition. *Angew. Chem. Int. Ed.* 2009; 48:7013–7016.
15. Pinner A. *Chem. Ber.* 1893; 26:2126.
16. Clavier G, Audebert P. s-Tetrazines as Building Blocks for New Functional Molecules and Molecular Materials. *Chem. Rev.* 2010; 110:3299–3314. [PubMed: 20302365]
17. Carboni RA, Lindsey RV. Reactions of Tetrazines With Unsaturated Compounds - A New Synthesis of Pyridazines. *J. Am. Chem. Soc.* 1959; 81:4342–4346.
18. Sauer J, et al. 1,2,4,5-tetrazine: Synthesis and reactivity in [4+2]cycloadditions. *Eur. J. Org. Chem.* 1998:2885–2896.
19. Thalhammer F, Wallfaher U, Sauer J. Reactivity of Simple Open-chain and Cyclic Dienophiles in Inverse-Type Diels-Alder Reactions. *Tetrahedron Lett.* 1990; 31:6851–6854.
20. Balcar J, Chrisam G, Huber FX, Sauer J. The Reactivity of Nitrogen Heterocyclics With Respect to Cyclooctyne as the Dienophile. *Tetrahedron Lett.* 1983; 24:1481–1484.
21. Wijnen JW, Zavarise S, Engberts JBFN, Charton M. Substituent effects on an inverse electron demand hetero Diels-Alder reaction in aqueous solution and organic solvents: Cycloaddition of substituted styrenes to di(2-pyridyl)-1,2,4,5-tetrazine. *J. Org. Chem.* 1996; 61:2001–2005.
22. Ciardiello F, Tortora G. EGFR antagonists in cancer treatment. *N Engl J Med.* 2008; 358:1160–1174. [PubMed: 18337605]
23. Sharma SV, Bell DW, Settleman J, Haber DA. Epidermal growth factor receptor mutations in lung cancer. *Nat Rev Cancer.* 2007; 7:169–181. [PubMed: 17318210]
24. Vincenzi B, Schiavon G, Silletta M, Santini D, Tonini G. The biological properties of cetuximab. *Crit Rev Oncol Hematol.* 2008; 68:93–106. [PubMed: 18676156]
25. Rachwal WJ, et al. Expression and activation of erbB-2 and epidermal growth factor receptor in lung adenocarcinomas. *Br J Cancer.* 1995; 72:56–64. [PubMed: 7599067]
26. Baskin JM, Bertozzi CR. Bioorthogonal click chemistry: Covalent labeling in living systems. *QSAR Comb. Sci.* 2007; 26:1211–1219.
27. Cole L, Davies D, Hyde GJ, Ashford AE. ER-Tracker dye and BODIPY-brefeldin A differentiate the endoplasmic reticulum and golgi bodies from the tubular-vacuole system in living hyphae of *Pisolithus tinctorius*. *J Microsc.* 2000; 197:239–249. [PubMed: 10692127]
28. Miller EW, Zeng L, Domaille DW, Chang CJ. Preparation and use of Coppersensor-1, a synthetic fluorophore for live-cell copper imaging. *Nat Protoc.* 2006; 1:824–827. [PubMed: 17406313]
29. Farinas J, Verkman AS. Receptor-mediated targeting of fluorescent probes in living cells. *J Biol Chem.* 1999; 274:7603–7606. [PubMed: 10075643]
30. Dumas-Verdes C, et al. BODIPY-Tetrazine Multichromophoric Derivatives. *Eur. J. Org. Chem.* 2010:2525–2535.
31. Nicolaou KC, W.M.D., Guy RK. Chemistry and Biology of Taxol. *Angew. Chem. Int. Ed.* 1994; 33:15–44.

32. Guy R, Scott Z, Sloboda R, Nicolaou K. Fluorescent taxoids. *Chem Biol.* 1996; 3:1021–1031. [PubMed: 9000007]
33. Mellado W, et al. Preparation and biological activity of taxol acetates. *Biochem Biophys Res Commun.* 1984; 124:329–336. [PubMed: 6548627]
34. Lee H, Sun E, Ham D, Weissleder R. Chip-NMR biosensor for detection and molecular analysis of cells. *Nat Med.* 2008; 14:869–874. [PubMed: 18607350]
35. Haun JB, Yoon TJ, Lee H, Weissleder R. Magnetic nanoparticle biosensors. *Wiley Interdiscip Rev Nanomed Nanobiotechnol.* 2010; 2:291–304. [PubMed: 20336708]
36. Lee H, Yoon TJ, Figueiredo JL, Swirski FK, Weissleder R. Rapid detection and profiling of cancer cells in fine-needle aspirates. *Proc Natl Acad Sci U S A.* 2009; 106:12459–12464. [PubMed: 19620715]
37. Ruenraroengsak P, Cook JM, Florence AT. Nanosystem drug targeting: Facing up to complex realities. *J Control Release.* 2010; 141:265–276. [PubMed: 19895862]
38. Haun JB, Devaraj NK, Hilderbrand SA, Lee H, Weissleder R. Bioorthogonal chemistry amplifies nanoparticle binding and enhances the sensitivity of cell detection. *Nat Nanotechnol.* 2010; 5:660–665. [PubMed: 20676091]
39. Haun JB, Devaraj NK, Marinelli BS, Lee H, Weissleder R. Probing Intracellular Biomarkers and Mediators of Cell Activation Using Nanosensors and Bioorthogonal Chemistry. *ACS Nano.* 2011
40. Green NM. Avidin and streptavidin. *Methods Enzymol.* 1990; 184:51–67. [PubMed: 2388586]
41. Haun JB, et al. Micro-NMR for rapid molecular analysis of human tumor samples. *Sci Transl Med.* 2011; 3:71ra16.
42. Han HS, et al. Development of a bioorthogonal and highly efficient conjugation method for quantum dots using tetrazine-norbornene cycloaddition. *J Am Chem Soc.* 2010; 132:7838–7839. [PubMed: 20481508]
43. Kelihier EJ, Reiner T, Turetsky A, Hilderbrand SA, Weissleder R. High-Yielding, Two-Step (18)F Labeling Strategy for (18)F-PARP1 Inhibitors. *ChemMedChem.* 2011
44. Li Z, et al. Tetrazine-trans-cyclooctene ligation for the rapid construction of 18F labeled probes. *Chem Commun (Camb).* 2010; 46:8043–8045. [PubMed: 20862423]
45. Reiner T, Earley S, Turetsky A, Weissleder R. Bioorthogonal small-molecule ligands for PARP1 imaging in living cells. *Chembiochem.* 2010; 11:2374–2377. [PubMed: 20967817]
46. Reiner T, Kelihier EJ, Earley S, Marinelli B, Weissleder R. Synthesis and In Vivo Imaging of a 18F-Labeled PARP1 Inhibitor Using a Chemically Orthogonal Scavenger-Assisted High-Performance Method. *Angew. Chem. Int. Ed.* 2011 In Press.
47. Goodwin DA, Meares CF. Advances in pretargeting biotechnology. *Biotechnol Adv.* 2001; 19:435–450. [PubMed: 14538068]
48. Rossin R, et al. In vivo chemistry for pretargeted tumor imaging in live mice. *Angew. Chem. Int. Ed.* 2010; 49:3375–3378.

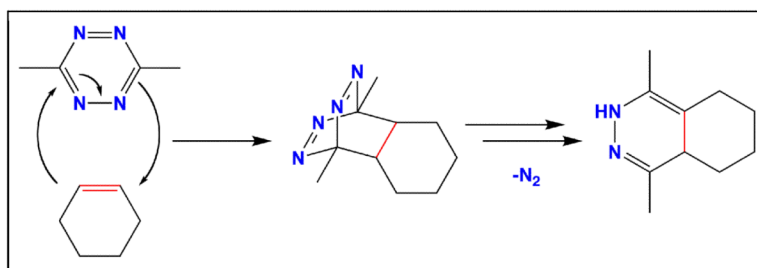


**Figure 1.**

An example of a tetrazine Diels-Alder cycloaddition. 1,2,4,5 Tetrazines such as 3,6-dimethyl-1,2,4,5-tetrazine can react with dienophiles such as alkenes and alkynes forming formal [4+2] Diels-Alder adducts. These adducts instantly undergo a retro Diels-Alder step, releasing nitrogen. In the case of alkenes, after rearrangement, isomeric dihydropyridazines are typically formed.



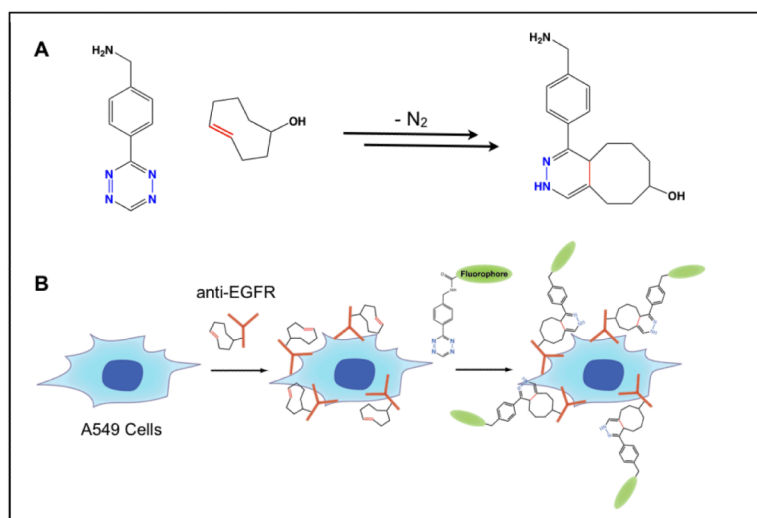


**Figure 2.**

A) reaction of benzylamino-tetrazine with *trans*-cyclooctenol is extremely rapid and leads to dihydropyridazine adducts. B) Live cell multistep labeling of A549 human lung carcinoma cells using tetrazine cycloadditions. Figure reproduced from Ref. [14] with permission from Wiley-VCH.

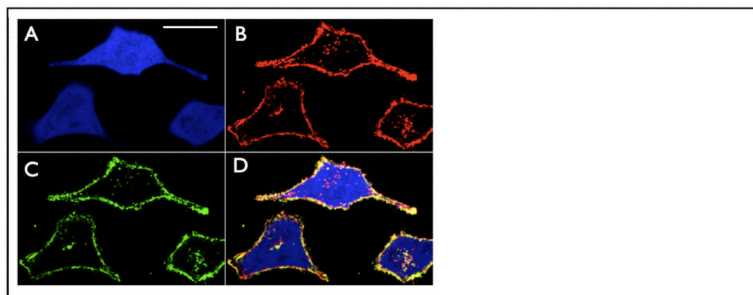


**Figure 3.** Confocal microscopy of Cetuximab pretargeted GFP-positive A549 lung cancer cells after tetrazine-fluorophore labeling. A) GFP channel. White scale bar in top left panel denotes 30 microns. B) Red channel: Cetuximab/*trans*-cyclooctene antibodies have also been directly labeled with AF555 and imaged in the rhodamine channel. C) Near-infrared channel showing the location of bound tetrazine near-infrared probe. D) Merge of GFP, red, and near-infrared channels. Figure reproduced from Ref. [14] with permission from Wiley-VCH.

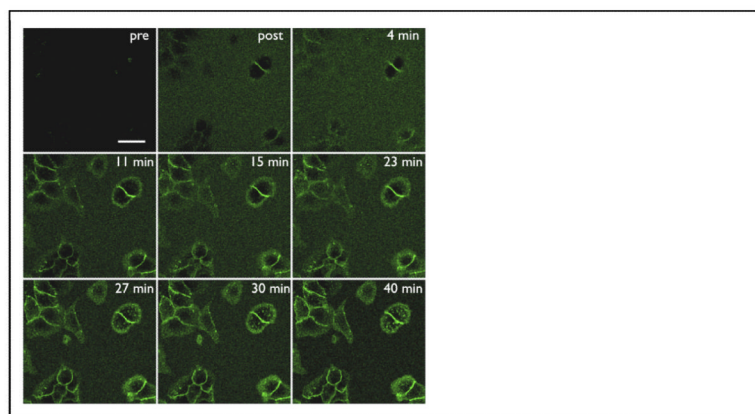


**Figure 4.**

Real time imaging of tetrazine labeling of pretargeted A549 cells. Cells were exposed to Cetuximab *trans*-cyclooctene, washed, and imaged in serum (FBS) using the near-IR channel (panel top left). The media was removed and immediately replaced with serum containing 50 nM tetrazine near-infrared probe (top middle panel). Images were taken periodically over 40 minutes. Scale bar in the top left panel denotes 30 microns. Figure reproduced from Ref. [14] with permission from Wiley-VCH.

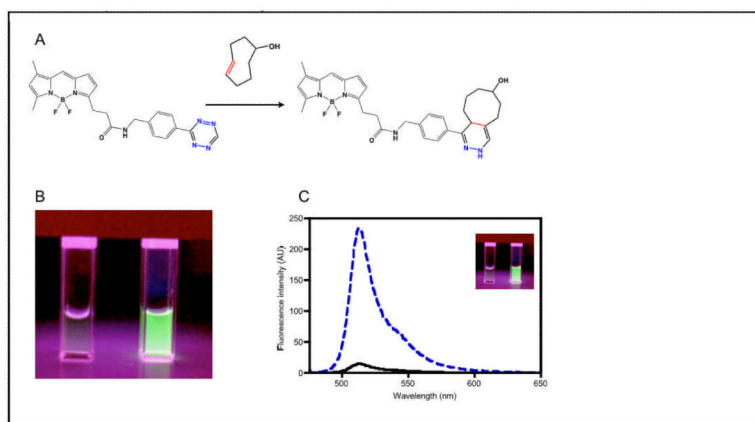


**Figure 5.**

A) Tetrazine-BODIPY FL reacts rapidly with *trans*-cyclooctenol via an inverse electron demand Diels-Alder cycloaddition to form isomeric dihydropyrazine products. B) Image comparing the visible fluorescence emission of tetrazine-BODIPY FL (left cuvette) to the corresponding dihydropyrazine products (right cuvette) under excitation from a handheld UV lamp. C) Emission spectra of tetrazine-BODIPY FL (black line) and the corresponding dihydropyrazine products (dashed blue line). Figure reproduced from Ref. [13] with permission from Wiley-VCH.

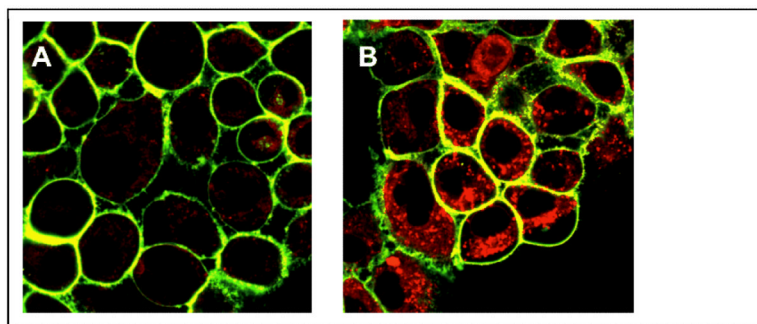


**Figure 6.** Confocal imaging of covalently labeled cell-surface bound and intracellular antibodies. A431 cells were exposed to 100 nM of *trans*-cyclooctene modified anti-EGFR antibody (Cetuximab). Cells were incubated for 1 hour at either 4°C (A) or 37°C (B) and subsequently labeled with 1  $\mu$ M of a highly charged tetrazine cyanine dye (green) and 1  $\mu$ M of a lipophilic tetrazine-BODIPY probe (red). Note the intracellular punctate stains representing internalized antibody.



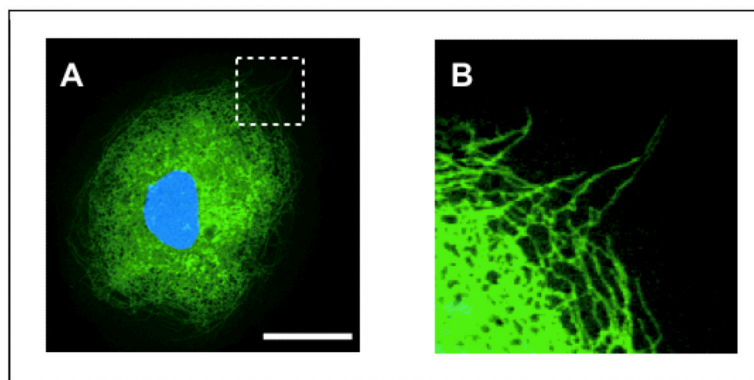


**Figure 7.**

A) Confocal microscopy of a kangaroo rat kidney cell after treatment with  $1\mu\text{M}$  *trans*-cyclooctene-taxol followed by  $1\mu\text{M}$  tetrazine-BODIPY FL (green). The nucleus is visualized using Hoechst stain (blue). Scale bar:  $30\mu\text{m}$ . Expansion of the section indicated by the dashed white line (B) reveals intracellular thread-like structures that are clearly stained and visible. Figure reproduced from Ref. [13] with permission from Wiley-VCH.

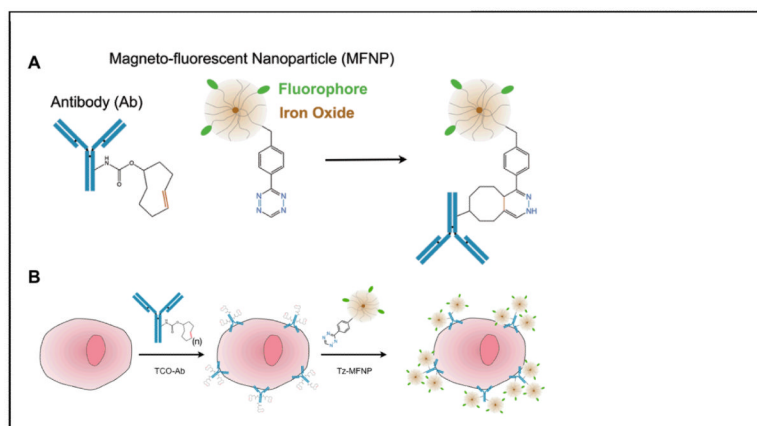


**Figure 8.**

A) Nanoparticle cycloaddition schematic showing the conjugation chemistry between a *trans*-cyclooctene modified antibody and tetrazine modified fluorescent iron-oxide nanoparticle. B) Multistep targeting of nanoparticles to specific cellular antigens through use of tetrazine cycloaddition chemistry. Figure reproduced from Ref. [38] with permission from the Nature Publishing Group.

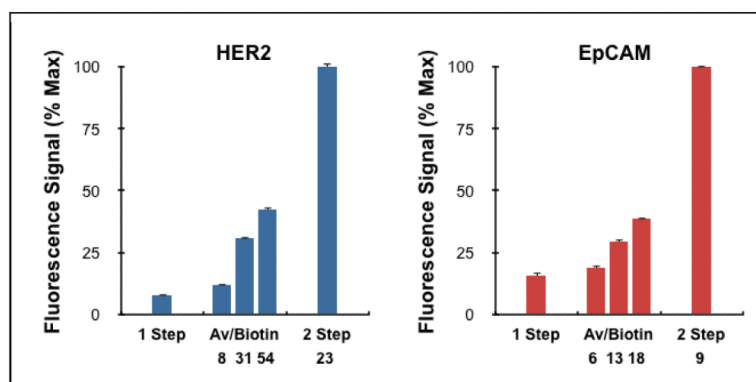


**Figure 9.** Comparison of different nanoparticle modification techniques for labeling either HER2 (left) or EpCAM (right) biomarkers. Fluorescence intensity of SK-BR-3 and HCT 116 cells labelled with 10 mg ml<sup>-1</sup> biotin-modified antibody and 100 nM avidin–MFNP was measured using flow cytometry. Biotinylated anti-HER2 and anti-EpCAM antibodies were prepared analogously to the *trans*-cyclooctene antibodies. Figure reproduced from Ref. [38] with permission from the Nature Publishing Group.

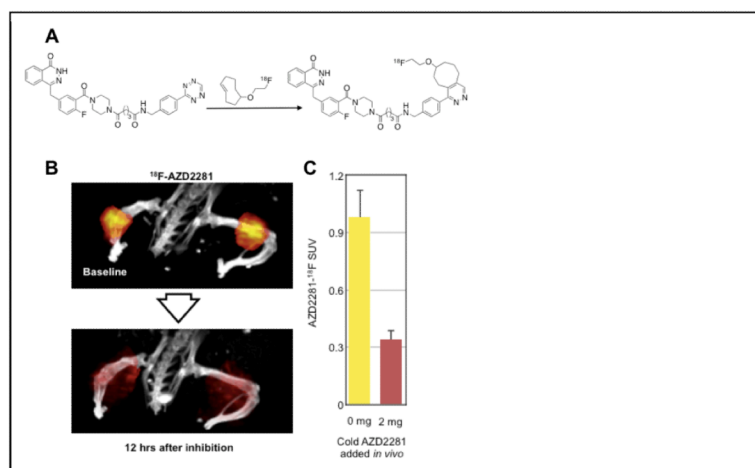


**Figure 10.**

A) Synthesis and structure of  $^{18}\text{F}$ -AZD2281 (only one product isomer shown) B) Three-dimensional reconstruction of a tumor-bearing animal injected with  $^{18}\text{F}$ -AZD2281 with and without pre-injection of AZD2281 (bladder segmented out for clarity). C) Quantification of uptake through the tumor in hind legs with and without intraperitoneal pre-injection of unlabeled AZD2281. SUV: standardized uptake value. Figure reproduced from Ref. [46] with permission from Wiley-VCH